

Sulfur surface chemistry on the platinum gate of a silicon carbide based hydrogen sensor

Yung Ho Kahng^{a)} and R. G. Tobin^{b)}

Department of Physics and Astronomy, Tufts University, Medford, Massachusetts 02155, USA

Reza Loloee and Ruby N. Ghosh

Department of Physics and Astronomy, Michigan State University, East Lansing, Michigan 48824, USA

(Received 7 March 2007; accepted 25 July 2007; published online 18 September 2007)

We have investigated the effects of sulfur contamination on a Pt-gate silicon carbide based field-effect gas sensor, under ultrahigh vacuum conditions, at a temperature of 527 °C. Exposure to hydrogen sulfide, even in the presence of hydrogen or oxygen at partial pressures of 20–600 times greater than the H₂S level, rapidly coated the gate with a monolayer of sulfur. Sulfur contamination reduced the magnitude of the sensor's response to alternating hydrogen and oxygen pulses by about 70%, as compared to the uncontaminated gate. There was no evidence of irreversible changes in device behavior due to sulfur deposition and removal. The adsorbed sulfur could not be removed by exposure to hydrogen at the pressures accessible. Oxygen was effective at removing the sulfur. The rate of sulfur oxidation was suppressed at high sulfur coverages, but not as strongly as on low-index single-crystal surfaces. These results are discussed in the context of prior experiments on Pt crystals and films. © 2007 American Institute of Physics. [DOI: 10.1063/1.2779288]

I. INTRODUCTION

Field-effect gas sensors based on metal-oxide-semiconductor (MOS) structures with catalytically active gates offer great promise as simple, inexpensive, versatile, and robust devices for the detection and measurement of hydrogen and other gases in a variety of applications.^{1,2} The first generation of these devices, based on silicon with palladium gates, was extensively investigated by Lundström and co-workers,^{3–9} and subsequent refinements have extended the capabilities of silicon-based devices and the understanding of their operation.^{10–12} The sensing mechanism involves several steps. (1) Dissociative adsorption of the analyte molecule on the surface of the gate, releasing hydrogen atoms; (2) diffusion of the H atoms to the metal/oxide interface, where they produce a dipole layer that shifts the capacitance-voltage (*C-V*) characteristic of the device toward more negative bias; (3) desorption of the hydrogen, either as H₂ or, in the presence of oxygen, as H₂O. The sensor signal is obtained by monitoring the chemically induced shift in device potential, at constant capacitance, as a function of hydrogen concentration.

Many practical applications for such a sensor, including automotive and power plant exhaust monitoring, solid-oxide fuel cells, and coal gasification, require operation at much higher temperatures than are possible with silicon devices, which are limited to temperatures below about 250 °C.¹³ Silicon carbide, with its high band gap, offers the possibility of operation at temperatures up to 1000 °C.^{2,13,14} SiC-based MOS devices have been demonstrated for monitoring automotive exhaust,^{15,16} flue gases from power plants,^{17–19} and selective catalytic reduction (SCR) in diesel engines.²⁰ Con-

siderable progress has been made in understanding the details of the sensing mechanism and interface properties of these devices.^{21–29} The surface chemistry of the catalytic gate, however, although it is crucial to device function, has received relatively little attention.^{21,25}

This work reports an ultrahigh vacuum (UHV) study of the surface chemistry of catalytic-gate silicon carbide MOS sensors, with a focus on sulfur contamination. Sulfur compounds are commonly present at the ppm level in many potential sensing applications, and sulfur is a notorious poison for catalytic reactions—and specifically for the dissociative adsorption of hydrogen—on transition metal surfaces.^{30–34} It is therefore important to determine whether sulfur contamination of the catalytic gate can occur, whether it affects sensor performance, and how it can be removed. We find that under UHV conditions sulfur contamination from hydrogen sulfide occurs readily, even in the presence of oxygen or hydrogen in the gas phase at levels much higher than that of the sulfide, and that the adsorbed sulfur adversely affects the device's response to alternating hydrogen and oxygen pulses. Under the conditions accessible to our experiments, the sulfur could not be removed by exposure to hydrogen, but heating in oxygen was very effective in removing sulfur. There was no evidence of irreversible changes in device behavior resulting from sulfur deposition and removal. In separate measurements at atmospheric pressure, exposure to 2000 ppm of hydrogen sulfide, followed by an extended exposure to oxygen, did not result in poisoning of the sensor's response to alternating pulses of hydrogen and oxygen.¹⁹

II. EXPERIMENTAL PROCEDURES

The experiments reported here were carried out on a single device, fabricated on a *n*-type 6H-SiC substrate (Cree, Inc.). The epitaxial layer was 3.6 μm thick with N dopant

^{a)}Present address: Korea Research Institute of Standards and Science, Yuseong, Daejeon 305-340, Republic of Korea.

^{b)}Electronic mail: roger.tobin@tufts.edu

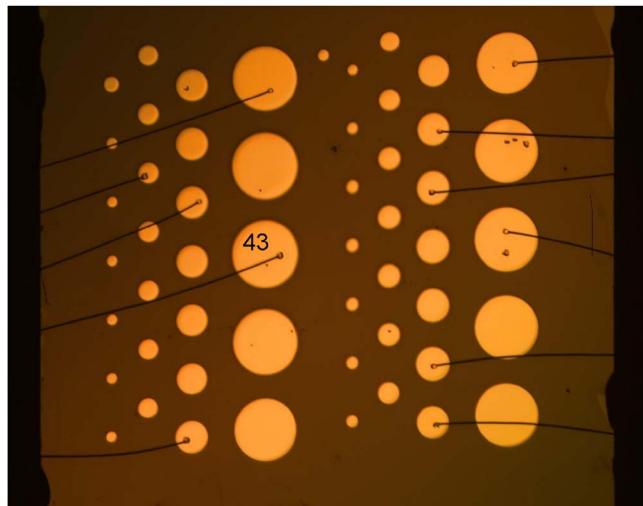


FIG. 1. (Color online) Micrograph of the wire-bonded gate surface of the sensor chip sample before activation. The nominal gate diameters are 200, 300, 500, and 1000 μm . All the sensor measurements reported here were measured on gate 43 (marked).

density of $2.1 \times 10^{16} \text{ N/cm}^3$. The SiO_2 layer was 39.5 nm thick and was grown by dry oxidation at 1150 $^\circ\text{C}$ followed by a 900 $^\circ\text{C}$ argon annealing and a 1175 $^\circ\text{C}$ NO annealing.³⁵ The catalytic gates were 100 nm thick platinum, grown by sputter deposition through a shadow mask at a sample temperature of 350 $^\circ\text{C}$ in 2.5 mTorr Ar. 52 circular Pt gates were deposited on a 1 cm^2 chip, with nominal diameters of 200, 300, 500, and 1000 μm . The back side of the sample was metallized using the same procedure. This deposition process yields continuous, nonporous gates in direct contact with the oxide.³⁶ As a result our devices differ, particularly in their response to gases other than hydrogen, from those described by other groups that use multilayer or porous Pt gates.^{17,19,20,25} Further details of the sample preparation can be found in Ref. 23.

After the gate deposition, the sample was mounted on an alumina header using silver paint (GC Electronics, Silver Print II), and 25 μm thick gold wire was wire bonded to selected gates and connected to gold pads on the header. The sample after wire bonding is shown in Fig. 1. All of the sensing experiments reported here were carried out on gate 43, with nominal diameter of 1000 μm , which is marked in Fig. 1.

As has been observed previously,^{14,18,21} the as-fabricated device showed little or no sensitivity to hydrogen. The sample was therefore “activated” by alternating exposures of 1% O_2 in N_2 (5 min) and 10% H_2 in N_2 (3 min) for 7 h at a flow rate of 40 SCCM (SCCM denotes cubic centimeter per minute at STP) while maintaining the device temperature at 610 $^\circ\text{C}$ (see Ref. 19 for experimental details). This procedure greatly enhances the performance of the sensor, through mechanisms that are not yet understood. One effect of the activation procedure is clearly a roughening of the Pt-gate surface that is visible both to the unaided eye and under the microscope.²⁴ Figure 2(a) shows a photomicrograph of one of the gates after activation; preactivation photographs taken under the same conditions appear shiny and featureless. Despite these dramatic changes in appearance, the surface com-

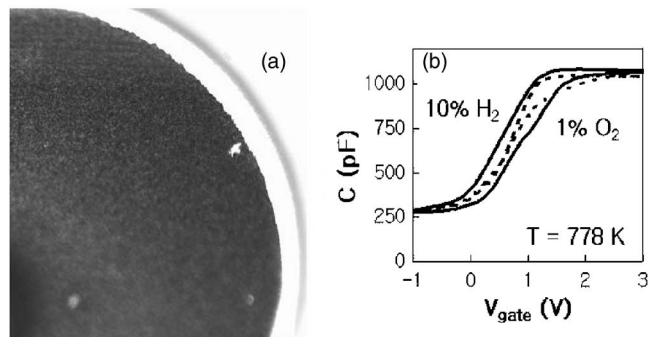


FIG. 2. Effects of gate activation. (a) Dark-field micrograph of a section of one of the gates after activation, showing the roughening of the surface. Before activation the gates are smooth and featureless, as shown in Fig. 1. (b) C - V curves of gate 43 before activation (dashed curves) and after activation (solid curves) measured at atmospheric pressure at a temperature of 505 $^\circ\text{C}$. The curves were scanned from positive gate voltage (accumulation) to negative (inversion) at a rate of 60 mV/s. In each set the curve on the right was measured in an atmosphere of 1% oxygen in N_2 and the curve on the left was measured in 10% hydrogen in N_2 ; the flow rate was 40 SCCM. The separation between the two curves represents the sensor response, which increases substantially after activation.

position as revealed by Auger electron spectroscopy (AES) remains pure Pt, and x-ray diffraction measurements show that the bulk crystal structure remains that of elemental platinum. The changes in the gate during activation therefore appear to be purely morphological, rather than changes in composition.

Figure 2(b) compares capacitance-voltage (C - V) curves measured at a sample temperature of 505 $^\circ\text{C}$ in 10% H_2 and 1% O_2 in nitrogen carrier gas at atmospheric pressure, before and after activation. Before activation the curves in H_2 and O_2 are nearly indistinguishable, while after activation a substantial voltage shift is observed. This shift provides the sensing response.

Following activation the sample was mounted in an ion-pumped ultrahigh vacuum chamber with a base pressure of $\sim 2 \times 10^{-10}$ Torr and cleaned by standard surface science methods: a combination of argon-ion sputtering and oxygen treatments (typically 10^{-7} Torr O_2 at a sample temperature of 525 $^\circ\text{C}$). Surface impurities were monitored by AES, carried out on an inactive gate to avoid possible electron-beam damage to the device. The lower trace in Fig. 3 shows a typical AES spectrum after cleaning. Oxygen (at 500 eV, not shown) and carbon (272 eV), the dominant contaminants, have been fully removed. A small amount (few at. %) of bismuth (101 eV) is visible, which probably comes from the gold wire and could not be fully removed. All other features in the spectrum are from platinum.

The upper trace in Fig. 3 shows an AES spectrum measured after exposure of the sample to hydrogen sulfide gas. The greatly enhanced peak at 152 eV is due to sulfur. Sulfur coverages (in monolayers; 1 ML=1 S per surface Pt atom) were determined from the relative peak-to-peak amplitudes of the 152 eV peak and the 237 eV Pt peak using the calibration of Bonzel and Ku.³⁷ The linearity of the sulfur Auger signal with coverage has been independently verified.³⁸

The sample assembly was heated by electron-beam bombardment, with the temperature monitored by a type-K ther-

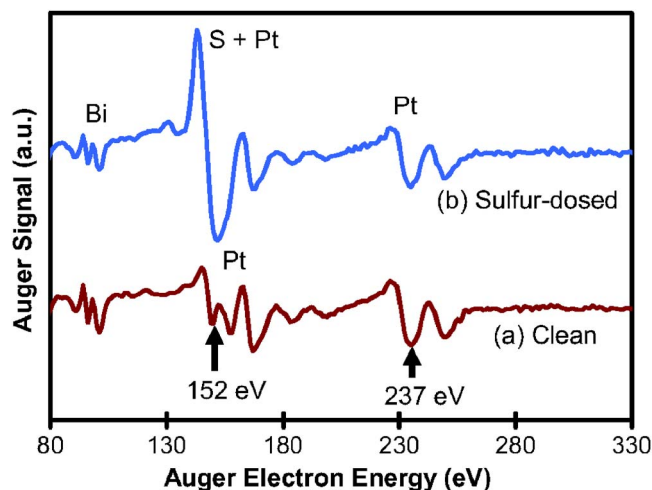


FIG. 3. (Color online) Auger spectra of Pt gate, (a) clean and (b) after exposure to hydrogen sulfide. The ratio of the peaks at 152 and 237 eV is used as a measure of sulfur coverage. The small peak at 101 eV indicates a small amount of bismuth on the surface. All of the other peaks are intrinsic to platinum.

mocouple attached to the alumina header with silver paint. A proportional-integral-derivative feedback system maintained the temperature within ± 1 °C during measurements. Electrical measurements were made *in situ* using a 1 MHz capacitance bridge. For sensor response measurements a feedback system varied the gate bias to keep the device at a constant capacitance, which was selected near the midgap point for optimum performance.²² Gases were introduced through separate leak valves. Hydrogen and hydrogen sulfide doses were carried out by backfilling the chamber, while oxygen was admitted through a multihole effusive doser³⁹ that enhanced the flux at the device by a factor of 14. Partial pressures were monitored using a quadrupole residual gas analyzer. Reported oxygen and hydrogen pressures have been corrected for doser enhancement (oxygen) and for analyzer sensitivity as determined by comparison with ionization gauge readings and published ion gauge sensitivity factors.⁴⁰ The analyzer sensitivity to hydrogen sulfide was estimated by comparing sulfur coverage to the gas exposure as measured by the integrated analyzer signal. From published sticking coefficient measurements for H_2S on Pt,^{31,34,37} we estimate that the analyzer sensitivity was ~ 0.01 A/Torr, roughly 100 times lower than for oxygen and hydrogen.

Figure 4 illustrates one cycle of a typical sensor response measurement. The sample is maintained at a constant temperature of 527 °C (800 K) and biased at a fixed capacitance of 450 pF, near the midgap point of the C - V curve [see Fig. 2(b)]. The graph shows the partial pressures of oxygen and hydrogen together with the gate voltage (note the inverted scale for the voltage) as a function of time. The sequence begins with the sample in an oxygen-rich environment to provide a hydrogen-depleted base line. The oxygen flow is then stopped, and hydrogen is introduced to a specified partial pressure. Because of the shift of the C - V curve to lower voltages shown in Fig. 2(b), the bias voltage must be reduced to maintain a constant capacitance. This bias shift, as indi-

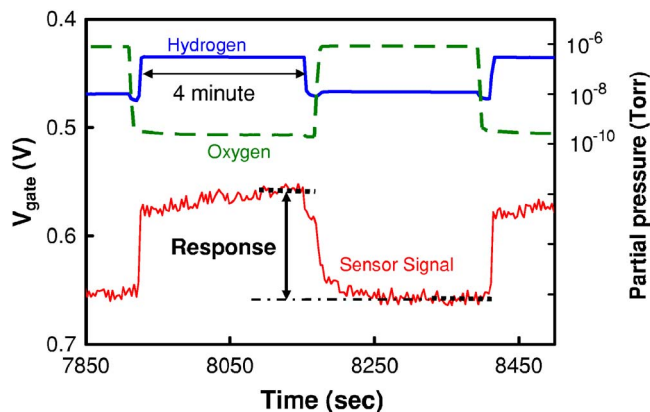


FIG. 4. (Color online) Example of a typical measurement of the sensor response to hydrogen in ultrahigh vacuum. H_2 (upper solid) and O_2 (dotted) partial pressures and sensor signal are plotted. The device was maintained at a constant capacitance of 450 pF by a feedback system and exposed alternately to hydrogen and oxygen; the gate voltage shift between the two conditions is taken to be the sensor response to the hydrogen pressure used. Partial pressures are indicated on the right axis and the sensor signal is indicated on the left axis (note the inverted scale). The device temperature was 523 °C (800 K).

cated in Fig. 2(b), is the sensor response. The hydrogen valve is then closed, oxygen is admitted to restore the hydrogen-depleted state, and the process is repeated.

Figure 5 shows a typical sequence of such measurement cycles, with varying hydrogen pressures, together with a plot of sensor response as a function of hydrogen pressure derived from the data. The device shows the Nernstian proportionality of sensor response to the logarithm of hydrogen pressure characteristic of electrochemical devices; for silicon-based devices this proportionality has been demonstrated over nine orders of magnitude.⁶ The observed sensitivity of 23 ± 3 mV/decade is smaller than observed in atmospheric pressure experiments for devices from the same fabrication run¹⁹ and smaller than observed for another device on the same chip in atmospheric pressure measurements carried out before the UHV studies (90 mV/decade). In addition, several months and many UHV gas and heating cycles after the measurements reported here, the same device showed sensitivity of about 90 mV/decade. The origin of these variations in sensitivity is not yet understood.

III. RESULTS AND DISCUSSION

A. Effects of sulfur on device response

At room temperature and above, hydrogen sulfide (H_2S) dissociates readily on clean platinum surfaces; the hydrogen then desorbs leaving adsorbed atomic sulfur on the surface.^{31,37,41,42} In view of sulfur's well-known tendency to suppress catalytic activity, through both site blocking and electronic effects,^{30–32,43,44} we expect exposure of the device to H_2S to reduce its response to hydrogen. Figure 6 demonstrates this effect. Figure 6(a) shows the response of the device, at 527 °C, to a sequence of alternating hydrogen and oxygen pulses similar to those shown in Figs. 4 and 5, before and immediately following a brief exposure to H_2S . The oxygen partial pressures were $\sim 10^{-10}$ Torr during the hydrogen pulses and $\sim 10^{-6}$ Torr between them, as in Fig. 4. Before

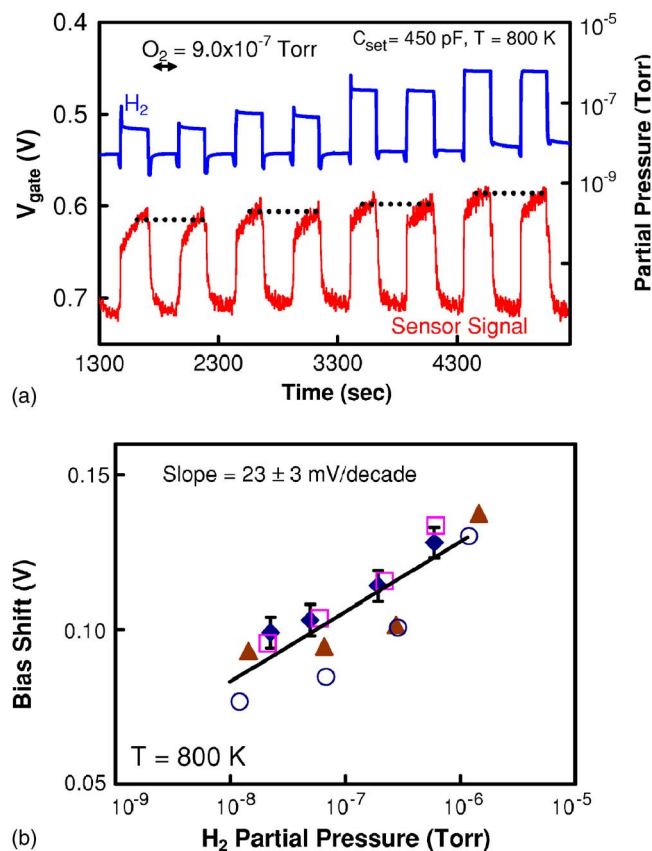


FIG. 5. (Color online) Signal and response to hydrogen for a clean sensor in UHV. (a) Gate voltage (sensor signal) at constant capacitance showing shifts in response to various partial pressures of hydrogen. Between hydrogen pulses oxygen was admitted at a partial pressure of 9×10^{-7} Torr. The H_2 partial pressures used were 5.6×10^{-8} , 1.2×10^{-7} , 4.8×10^{-7} , and 1.5×10^{-6} Torr, with two pulses at each pressure. The dashed lines indicate the sensor responses. (b) Sensor response as a function of hydrogen partial pressure. The symbols indicate the results of four independent measurements; the error bars shown are typical of all four sets. The voltage shift is proportional to the logarithm of the hydrogen partial pressure, with a slope of 23 ± 3 mV/decade.

the start of the experiment, AES showed that the gate surface was free of sulfur and other contaminants. Immediately after the H_2S dose AES showed a sulfur coverage of 0.38 ML.

For the first two oxygen/hydrogen cycles following sulfur deposition (indicated with arrows), the gate voltage shift between the hydrogen and oxygen pulses is reduced by a factor of ~ 3 compared to the response to similar pulses on the clean surface. This point is emphasized in Fig. 6(b), which highlights hydrogen pulses of comparable magnitude before and immediately after sulfur deposition. The primary reason for the reduced response is that the first two oxygen exposures do not bring the bias back to its base line level of about 0.7 V. This observation suggests that adsorbed sulfur interferes with the surface reactions by which oxygen removes hydrogen from the sensing interface, possibly by impeding the dissociation of oxygen molecules.

The third oxygen pulse restores the device to its base line condition, and subsequent sensor responses are comparable to those observed before the sulfur was deposited. An AES spectrum measured after the complete measurement sequence showed no detectable sulfur on the surface.

This experiment demonstrates (1) that sulfur is deposited on the surface by exposure to H_2S , (2) that the deposited sulfur suppresses the sensor response, (3) that the sulfur is readily removed by exposure to oxygen, and (4) that after the sulfur is removed the device response returns to its original level—there are no irreversible changes resulting from the deposition and removal of sulfur. The effectiveness of oxygen at removing sulfur, while desirable from a device standpoint, makes it difficult to obtain a meaningful quantitative measure of sulfur's effect on device sensitivity, since the hydrogen/oxygen cycling required for sensitivity measurements rapidly removes the sulfur.

The change in sensor response due to sulfur is apparently due to modification of the gate surface chemistry, not to changes in the electronic properties of the device. Figure 7 shows two C - V curves, both measured in UHV at the chamber's base pressure of 2×10^{-10} Torr (predominantly hydrogen). One is of the device with a clean gate (as established by AES) and the other of the device when the gate was contaminated with 0.45 ML of sulfur. The curves are indistinguishable. Evidently, sulfur itself does not produce a sensor response, nor does it modify the C - V characteristic of the device.

B. Sulfur adsorption in the presence of oxygen and hydrogen

In sensing applications hydrogen sulfide is rarely the dominant gas. More commonly it is a minor impurity in a gas stream with much higher concentrations of oxygen and/or hydrogen. Since both gases can react with sulfur (to form SO_2 and H_2S , respectively, among other species), it is of interest to determine whether their presence in the gas stream inhibits sulfur contamination. We carried out a series of experiments in which the clean sample, held at 527 °C, was exposed simultaneously to H_2S at partial pressures from 10^{-8} to 10^{-5} Torr and to O_2 or H_2 at pressures of 4–20 times higher in the case of oxygen, or 6–600 times higher in the case of hydrogen. Although the absolute partial pressures in these experiments are many orders of magnitude lower than would be encountered in practical sensing applications, the partial pressure *ratios* are in a range that is relevant to applications.

The number of incident H_2S molecules per unit area was estimated from the H_2S partial pressure integrated over the exposure time.⁴⁵ Following the exposure the sulfur coverage was determined from AES and a relative sticking coefficient (sulfur atoms adsorbed per incident H_2S molecule) was calculated. Lacking an independent partial pressure calibration, we could not determine the absolute sticking coefficient, so our values are normalized to the sticking coefficient at the lowest accessible hydrogen and oxygen pressures. Other measurements of H_2S dissociation on Pt, however, suggest that the sticking coefficient in the absence of other gases is between 0.5 and 1.0.^{31,37,38} In some cases (shown with horizontal bars), the final AES measurement showed that the sulfur coverage had already reached its saturation value. The computed sticking coefficient must then be viewed as a lower limit, since extending the exposure beyond saturation

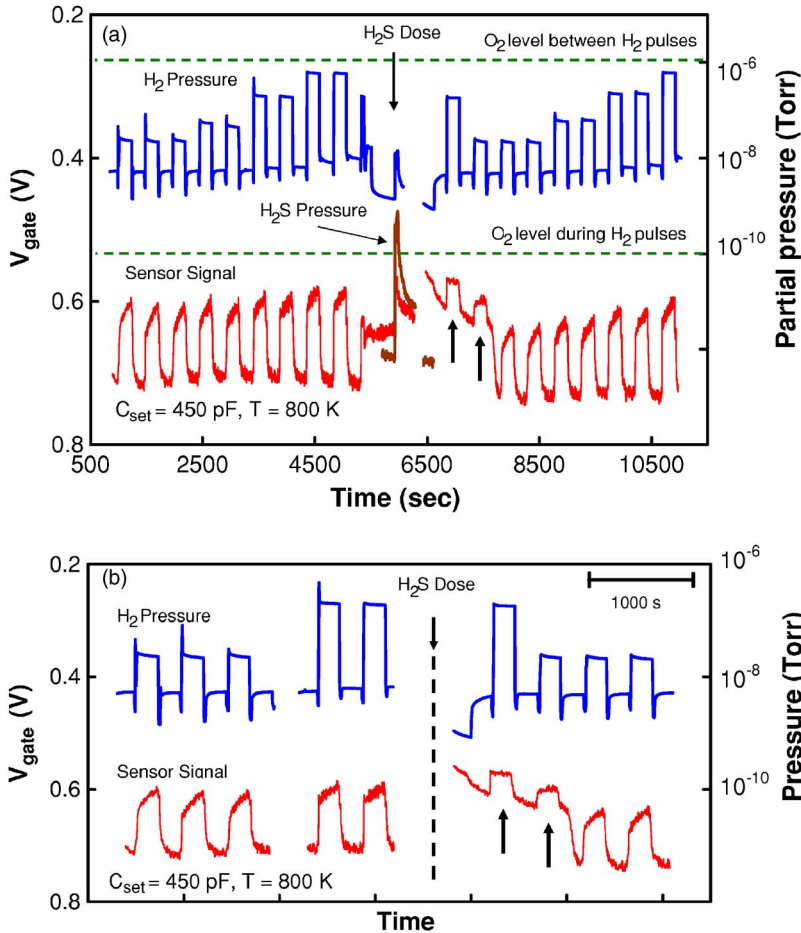


FIG. 6. (Color online) The effect of sulfur on the sensor response, in UHV. (a) Sensor response to a sequence of alternating hydrogen and oxygen pulses, starting from a clean sample, before and after exposure to a pulse of hydrogen sulfide. An AES spectrum immediately after the H_2S dose showed a sulfur coverage of 0.4 ML. For the first two hydrogen pulses after the H_2S dose (indicated with arrows), the sensor's voltage shift is reduced by $\sim 70\%$ compared to the clean gate. After the third pulse, the sensor returned to its clean-gate behavior. An AES spectrum at the end of the sequence found no detectable sulfur on the surface. (b) Selected hydrogen pulses from (a) before and after the H_2S dose, with comparable hydrogen pressures.

increases the number of molecules per unit area incident on the surface without affecting the sulfur coverage.

The data are shown in Fig. 8. Over the range of pressures studied, hydrogen had no observable effect on sulfur adsorption. Oxygen, however, strongly interfered with sulfur accumulation, reducing the sticking coefficient by a factor of

10^3 at an O_2 pressure of $\sim 4 \times 10^{-5}$ Torr. Evidently sulfur oxidation competes significantly with sulfur adsorption under these conditions.

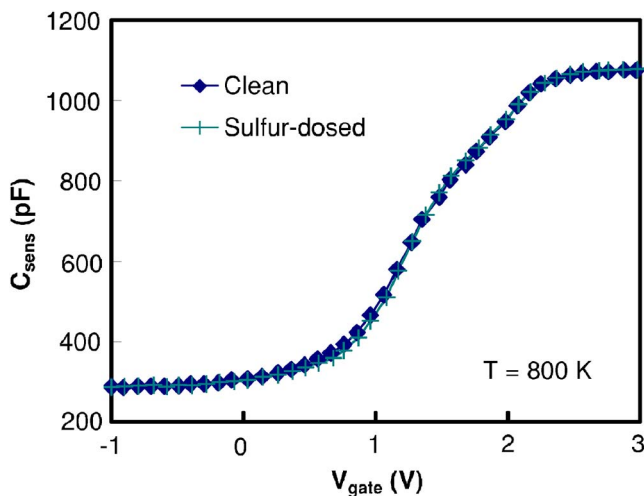


FIG. 7. (Color online) Capacitance-voltage (C - V) curves measured on the same device with a clean and sulfur-contaminated (0.45 ML S) gate surface, in UHV ($\sim 10^{-10}$ Torr). Both curves were scanned from positive (accumulation) to negative (inversion) gate voltage, at a rate of 100 mV/s. The curves are indistinguishable within experimental error.

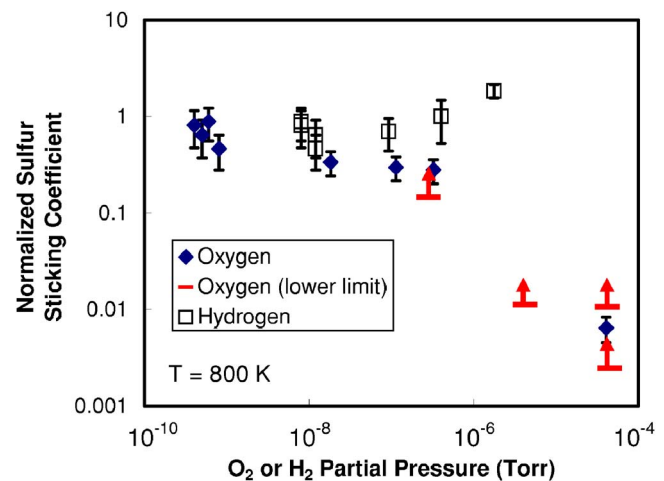


FIG. 8. (Color online) Effect of oxygen and hydrogen on the deposition of sulfur by exposure to H_2S at 527 °C. Sticking coefficient (S adsorbed per incident H_2S molecule) of H_2S to the Pt gate in O_2 and H_2 background pressures, normalized to the value at the lowest background pressure. The horizontal bars with arrows represent lower limits; in these measurements the surface was saturated with sulfur after the H_2S exposure, as discussed in the text. Hydrogen has virtually no effect, while oxygen significantly suppresses, but does not prevent sulfur deposition. These experiments include O_2/H_2S partial pressure ratios up to ~ 20 and H_2/H_2S ratios up to ~ 600 .

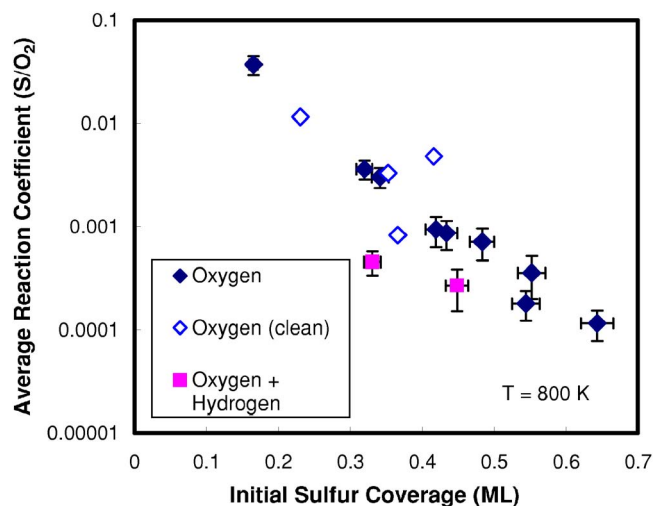


FIG. 9. (Color online) Average reaction coefficient (S atoms removed per incident O_2 molecule) as a function of initial S coverage. The oxygen partial pressure was $\sim 1 \times 10^{-6}$ Torr and the sample temperature was 527 °C. The open symbols designate experiments in which all sulfur was removed from the surface. The squares indicate experiments in which a hydrogen partial pressure of 7×10^{-7} Torr was introduced in addition to the oxygen.

The greatest suppression of sulfur adsorption occurs at the highest O_2 pressure, which did not correspond to the highest O_2/H_2S ratio: for O_2 pressures of about 4×10^{-5} Torr the ratio was in the range of 4–6, while higher ratios (~ 20) were obtained for some experiments with oxygen pressures in the 10^{-7} – 10^{-6} Torr range. These results suggest that under our experimental conditions the oxygen coverage on the surface, which determines the rate of sulfur removal, is controlled more by thermal desorption of oxygen than by reaction of oxygen with sulfur.

C. Removal of adsorbed sulfur with hydrogen and oxygen

Since it is clear that sulfur accumulation on the gate surface is likely to occur and can have adverse effects on sensor performance, it is important to determine whether, and under what conditions, the sulfur can be removed. To this end we deposited various coverages of sulfur by exposure to H_2S , and then exposed the sample at 527 °C to oxygen or hydrogen at various pressures and for various times. Sulfur coverages before and after treatment were determined from the AES spectrum. For the oxygen exposure experiments, the number of oxygen molecules per unit area incident on the surface was determined from the oxygen partial pressure and exposure time. The ratio of the change in sulfur coverage to the number of incident oxygen molecules gives the average reaction coefficient, defined as the average number of sulfur atoms removed per incident O_2 molecule.

Figure 9 shows the average reaction coefficient for oxygen exposure as a function of the initial sulfur coverage. Within experimental error the average reaction coefficient decreases exponentially with sulfur coverage. Extrapolating to zero coverage gives a rate of about 0.2 S/ O_2 , while at the highest coverages the reaction probability decreases to $\sim 10^{-3}$.

Some care is required in interpreting these data. As we discuss in the next section, adsorbed sulfur interferes with the dissociative adsorption of oxygen, so the actual reaction probability depends very strongly on the instantaneous sulfur coverage, and even on the treatment history of the sample, which can affect the distribution of sulfur on the surface.^{43,46,47} If a surface with a high sulfur coverage is exposed to a constant oxygen pressure, very little change in sulfur coverage occurs for several minutes; then as openings begin to appear in the sulfur layer the reaction rate accelerates dramatically, and the majority of the sulfur is removed within the last few seconds. This highly nonlinear behavior, which has also been reported in single-crystal studies,^{43,46,47} explains the abrupt reappearance of the sensor response after two hydrogen/oxygen cycles following sulfur exposure in Fig. 6.

Because the reaction probability depends so strongly on coverage, however, the measured *average* reaction rate shown in Fig. 9 depends not only on the initial sulfur coverage but also on the length of oxygen exposure and extent of sulfur removal. For high initial coverages, a short oxygen exposure, during which the sulfur coverage changes only slightly, will measure a lower average rate than a longer exposure in which the coverage decreases enough for the rapid reaction conditions to be reached. The maximum average rate, for a given initial coverage, will be observed if the oxygen exposure is terminated just as the sulfur coverage reaches zero. But if the oxygen exposure is continued after the surface is clean, that extra exposure will tend to reduce the measured average rate, since it is computed by dividing the change in sulfur coverage by the oxygen exposure. The open symbols in Fig. 9 represent experiments in which all sulfur was removed from the surface, and lie both above and below the data for experiments in which the sulfur was only partially removed because of the competition between these two effects.

From the standpoint of sensor operation, however, it is important that even at the highest sulfur coverages attainable, the surface could be completely cleaned of sulfur by exposure to $\sim 10^{-4}$ Torr O_2 for several minutes and that the performance of the device after sulfur removal was indistinguishable from its performance before exposure to H_2S .

The squares in Fig. 9 show the sulfur removal rate when the oxygen treatment was accompanied by a constant background pressure of 7×10^{-7} Torr hydrogen, comparable to the oxygen pressure. These two measurements suggest that hydrogen may reduce the rate at which oxygen removes sulfur from the surface, probably because the hydrogen reacts with some of the oxygen to form water.

Figure 10 shows the variation of the sensor signal (gate bias at constant capacitance) during three cycles of oxygen treatment of a gate initially saturated with adsorbed sulfur. As in Fig. 6, no change in bias is observed until just before the end of the second oxygen treatment. At that point the sulfur coverage had been reduced from 0.6 to 0.5 ML. From that point, however, the cleaning proceeds very rapidly, as indicated by the abrupt bias shift when the third oxygen treatment is initiated. At the end of the third treatment, the AES spectrum showed no detectable sulfur.

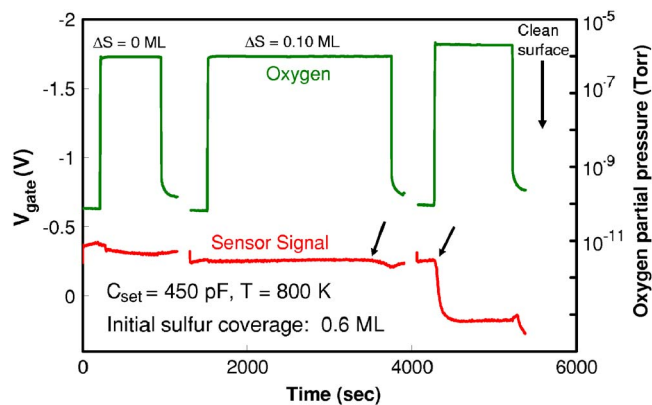


FIG. 10. (Color online) Variation of the sensor signal during oxygen cleaning of a sulfur-saturated sample (initial S coverage of 0.60 ML), showing the slow onset of cleaning followed by a very rapid reaction once some of the sulfur is removed. Three cycles of oxygen treatment are shown, with AES measurements between them to determine changes in the sulfur coverage. Because the sensing feedback is interrupted for the Auger measurements, the small voltage shifts *between* doses are less significant than the changes *during* a dose. No significant change in the gate voltage is observed until the point marked by the first arrow. The oxygen was then immediately shut off and the sulfur coverage measured with AES and found to have decreased by 0.1 ML. When oxygen was again introduced the sensor signal changed very rapidly, as indicated by the second arrow, and after the third oxygen treatment AES showed a completely clean surface.

In a separate experiment at atmospheric pressure, an identically fabricated sensor was exposed to a pulse of 2000 ppm H_2S in 10% H_2 (balance nitrogen).¹⁹ Following an extended oxygen exposure, the device showed no degradation in its response to alternating pulses of hydrogen and oxygen. These results are consistent with our observation that any sulfur deposited on the surface is readily removed by exposure to oxygen.

Similar tests using hydrogen rather than oxygen showed no cleaning effect. Figure 11 shows the variation of the sulfur coverage after a series of hydrogen treatments, for three initial sulfur coverages. In no case was a meaningful reduction in sulfur level observed. We can set an upper limit on the reaction coefficient of $\sim 3 \times 10^{-5}$ S/ H_2 , two to three orders of magnitude lower than for oxygen at comparable sulfur coverages.

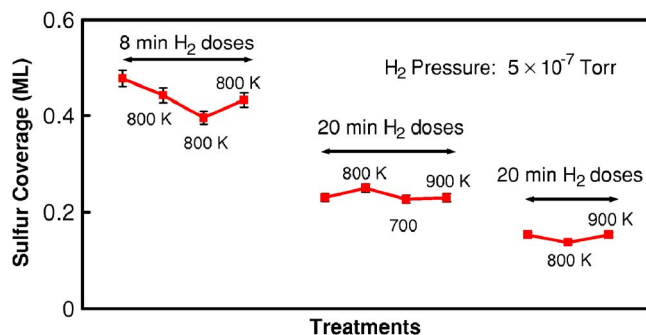


FIG. 11. (Color online) Variation of sulfur coverage with hydrogen treatment. Each treatment consisted of exposing the sample to 5×10^{-7} Torr H_2 for the time and at the temperature indicated. Three different initial sulfur coverages were investigated. Within experimental error no significant removal of sulfur was observed.

D. Discussion

The data presented here demonstrate that adsorbed sulfur has a serious adverse effect on the sensitivity of platinum-gate silicon carbide gas sensors, so that methods of preventing or removing sulfur contamination will be essential in applications where sulfur compounds are present in the gas stream. Three broad conclusions can be drawn regarding the surface chemistry of sulfur on the activated platinum gate.

- (1) Hydrogen sulfide dissociates readily on the surface, leaving behind a stable layer of adsorbed sulfur.
- (2) Hydrogen gas has little effect either in inhibiting sulfur deposition or in removing the sulfur once it is deposited.
- (3) The adsorbed sulfur is readily oxidized by oxygen at 527 °C, so that ambient oxygen significantly inhibits sulfur accumulation, and a sulfur-contaminated surface can be fully cleaned by exposure to oxygen. The sulfur removal rate, however, decreases strongly with increasing sulfur coverage.

These results are broadly consistent with previous investigations of sulfur chemistry on single-crystal platinum surfaces, with some subtle but significant differences, which are probably attributable to the roughness of the gate and the correspondingly high concentration of defect sites. Sensor studies at atmospheric pressure have not shown a poisoning effect due to sulfur, probably because it is so effectively removed by oxygen.

Single-crystal studies have consistently found that the deposition of adsorbed sulfur from hydrogen sulfide occurs with high probability on clean Pt surfaces at room temperature and above. A first-principles theoretical study by Michaelides and Hu found the dissociative adsorption reaction $\text{H}_2\text{S}(\text{gas}) \rightarrow \text{S}(\text{ads}) + 2\text{H}(\text{ads})$ to be exothermic by 2.8 eV/mol, with activation barriers of less than 0.1 eV.⁴⁸ Sticking coefficients at low sulfur coverage have been estimated in the range of 0.5–1.0,^{31,37,38} and the maximum sulfur coverages attainable are typically in the range of 0.5–0.65 ML, depending on the crystal face, temperature, and amount of gas dosing.^{31,37,41} In these respects the behavior of the activated Pt gate strongly resembles that of single-crystal samples.

The ineffectiveness of hydrogen in either preventing or reversing sulfur contamination is also consistent with theoretical predictions and single-crystal studies. On Pt(111) Michaelides and Hu found the formation of HS from coadsorbed H and S to be endothermic by 1.23 eV, with a further endothermicity of 0.90 eV for the formation of H_2S .⁴⁸ Not surprisingly, then, H_2S formation from adsorbed sulfur and hydrogen gas is not observed experimentally on either Pt single crystals or polycrystalline Pt foil.^{44,49} From our results it appears that the roughness and corresponding high surface defect concentration of the activated gate do not appreciably change the unfavorable energetics for the removal of adsorbed sulfur by hydrogen. It should be noted, however, that our experiments used very low hydrogen pressures ($\sim 5 \times 10^{-7}$ Torr). Successful regeneration of sulfur-poisoned Pt catalysts by exposure to 300 Torr H_2 for 4 h at 500 °C has been reported,⁵⁰ and we cannot rule out the possibility that

similarly aggressive hydrogen treatments would be successful in cleaning sulfur from our sensors as well.

Studies of sulfur oxidation on Pt consistently find that it proceeds by a Langmuir-Hinshelwood reaction between adsorbed S and SO and adsorbed oxygen atoms; dissociative adsorption of oxygen from the gas phase is therefore an essential first step in the reaction.^{43,46-51} Even low coverages of sulfur strongly suppress the adsorption of oxygen,^{31,43,46,47} resulting in a strong suppression of the oxidation reaction with increasing sulfur coverage similar to the behavior we observe in Fig. 9. Köhler *et al.* reported that the sticking coefficient of oxygen on Pt(111) becomes effectively zero above a sulfur coverage of only 0.09 ML.⁴⁶ Even at higher sulfur coverages, however, the sulfur oxidation rate was not zero because thermal fluctuations in the sulfur overlayer occasionally produce open sites for oxygen dissociation, but it was much lower than in our measurements. Their data for a sulfur coverage of 0.24 ML and a sample temperature of 770 °C, for example, correspond to an average reaction coefficient of less than 3×10^{-4} S/O₂, more than a factor of 10 smaller than in our data, even though our experiment was carried out at a lower temperature, so that the thermally activated openings in the sulfur layer should be less frequent. Astegger and Bechtold also reported that at 0.33 ML coverage, the sulfur overlayer was unaffected by repeated oxygen exposures; these experiments, however, were carried out at lower temperature (47 °C), which could account for the low reaction rate.⁴⁷ In contrast to these results, on the more open Pt(110) surface Bonzel and Ku observed a reaction rate of ~ 0.01 S/O₂ for an initial sulfur coverage of 0.38 ML at 200 °C, higher than we observed at similar coverages in Fig. 9, though still much lower than the rate they measured at low sulfur coverage.⁴³

The dissociative adsorption of oxygen on platinum surfaces is highly structure sensitive, occurring far more readily at low-coordination sites such as steps and defects than on the flat terraces of low-index single-crystal surfaces.⁵²⁻⁵⁵ We suggest that the macroscopic roughness of the activated gate reflects a high density of atomic-scale surface defects, which accounts for the ability of oxygen to remove even very high sulfur coverages at a rate much higher than one would expect from measurements on the close-packed Pt(111) surface. Either these surface defect sites are not effectively blocked by adsorbed sulfur or the mobility of the sulfur on the defect sites is enhanced, so that the random formation of open sites by thermal fluctuations occurs more rapidly than on the close-packed surface. Measurements of the temperature dependence of the reaction would help us to elucidate the mechanism. In any case the relatively facile removal of adsorbed sulfur by oxygen exposure is advantageous for sensing applications.

E. Conclusion

Sulfur poisoning is a potentially serious problem for gas sensors that rely on a catalytic metal gate for their operation. While the extensive studies of sulfur chemistry on platinum single crystals, smooth polycrystalline films, and oxide-supported dispersed catalysts provide valuable guidance, the

preparation, structure, and function of the sensor gate are sufficiently different that it is important to investigate its properties. Our results show that sulfur adsorbed from hydrogen sulfide gas has a serious detrimental effect on the response of the silicon carbide based sensor tested to alternating pulses of hydrogen and oxygen in UHV, reducing the magnitude of the gate voltage shift at constant capacitance by $\sim 70\%$. However, the performance of the device after sulfur removal was indistinguishable from its performance before exposure to H₂S. The presence of background oxygen or hydrogen at levels up to ~ 20 times (for oxygen) or ~ 600 times (for hydrogen) greater than the hydrogen sulfide pressure had little effect on sulfur contamination. It was not possible to remove the deposited sulfur by exposure to hydrogen at pressures in the 10^{-7} Torr range. Sulfur could be removed by exposure to oxygen, but at high sulfur coverages the reaction rate was very low. These results are broadly consistent with prior studies of smooth platinum surfaces.

ACKNOWLEDGMENTS

This report was prepared with the support of the U.S. Department of Energy, under Award No. DE-FC26-03NT41847. However, any opinions, findings, conclusions, or recommendations expressed herein are those of the authors and do not necessarily reflect the views of the DOE. The authors thank Peter Tobias, currently at Honeywell, for his assistance and advice, and V. H. S. Moorthy for preliminary experiments. The gate oxidation was performed by John Williams, Department of Physics, Auburn University.

- ¹G. Müller, G. Krötz, and J. Schalk, *Phys. Status Solidi A* **185**, 1 (2001).
- ²A. Lloyd Spetz, P. Tobias, A. Baranzahi, P. Mårtensson, and I. Lundström, *IEEE Trans. Electron Devices* **46**, 561 (1999).
- ³I. Lundström, S. Shivaraman, C. Svensson, and L. Lundkvist, *Appl. Phys. Lett.* **26**, 55 (1975).
- ⁴K. I. Lundström, M. S. Shivaraman, and C. M. Svensson, *J. Appl. Phys.* **46**, 3876 (1975).
- ⁵I. Lundström, *Sens. Actuators* **1**, 403 (1981).
- ⁶H. M. Dannelun, L.-G. Petersson, D. Söderberg, and I. Lundström, *Appl. Surf. Sci.* **17**, 259 (1984).
- ⁷L.-G. Petersson, H. M. Dannelun, and I. Lundström, *Phys. Rev. Lett.* **52**, 1806 (1984).
- ⁸L.-G. Ekedahl, M. Eriksson, and I. Lundström, *Acc. Chem. Res.* **31**, 249 (1998).
- ⁹L.-G. Petersson, H. M. Dannelun, J. Fogelberg, and I. Lundström, *J. Appl. Phys.* **58**, 404 (1985).
- ¹⁰P. Kreisl, A. Helwig, G. Müller, E. Obermeier, and S. Sotier, *Sens. Actuators B* **106**, 442 (2005).
- ¹¹P. Kreisl, A. Helwig, A. Friedberger, G. Müller, E. Obermeier, and S. Sotier, *Sens. Actuators B* **106**, 489 (2005).
- ¹²A. Salomonsson, M. Eriksson, and H. Dannelun, *J. Appl. Phys.* **98**, 014505 (2005).
- ¹³A. Baranzahi, A. Lloyd Spetz, B. Andersson, and I. Lundström, *Sens. Actuators B* **26-27**, 165 (1995).
- ¹⁴A. Lloyd Spetz, A. Baranzahi, P. Tobias, and I. Lundström, *Phys. Status Solidi A* **162**, 493 (1997).
- ¹⁵H. Wingbrant, H. Svenningstorp, P. Salomonsson, P. Tengström, I. Lundström, and A. Lloyd Spetz, *Sens. Actuators B* **93**, 295 (2003).
- ¹⁶H. Svenningstorp, B. Widén, P. Alomsonsson, L.-G. Ekedahl, I. Lundström, P. Tobias, and A. Lloyd Spetz, *Sens. Actuators B* **77**, 177 (2001).
- ¹⁷A. Lloyd Spetz, L. Unéus, H. Svenningstorp, P. Tobias, L.-G. Ekedahl, O. Larsson, S. Savage, C. Harris, P. Mårtensson, R. Wigren, P. Salomonsson, B. Häggendahl, P. Ljung, M. Mattsson, and I. Lundström, *Phys. Status Solidi A* **185**, 15 (2001).
- ¹⁸M. Andersson, P. Ljung, M. Mattson, M. Löfdahl, and A. Lloyd Spetz, *Top. Catal.* **30/31**, 365 (2004).

- ¹⁹R. Loloee, B. Chorpening, S. Beer, and R. N. Ghosh, *Sens. Actuators B* (2007).
- ²⁰H. Wingbrant, H. Svenningstorp, P. Salomonsson, D. Kubinski, J. H. Visser, M. Löfdahl, and A. Lloyd Spetz, *IEEE Sens. J.* **5**, 1099 (2005).
- ²¹H. Wingbrant and A. Lloyd Spetz, *Appl. Surf. Sci.* **252**, 7473 (2006).
- ²²P. Tobias, B. Golding, and R. N. Ghosh, *IEEE Sens. J.* **2**, 543 (2003).
- ²³R. N. Ghosh and P. Tobias, *J. Electron. Mater.* **34**, 345 (2005).
- ²⁴A. Samman, S. Gebremariam, L. Rimai, X. Zhang, J. Hangan, and G. W. Auner, *Sens. Actuators B* **63**, 91 (2000).
- ²⁵J. Schalwig, P. Kreisl, S. Ahlers, and G. Müller, *IEEE Sens. J.* **2**, 294 (2002).
- ²⁶S. Nakagomi, A. Lloyd Spetz, I. Lundström, and P. Tobias, *IEEE Sens. J.* **2**, 379 (2002).
- ²⁷S. Kandasamy, A. Trinchi, W. Wlodarski, E. Comini, and G. Sberveglieri, *Sens. Actuators B* **111–112**, 111 (2005).
- ²⁸M. Wallin, H. Grönbeck, A. Lloyd Spetz, and M. Skoglundh, *Appl. Surf. Sci.* **235**, 487 (2004).
- ²⁹M. Wallin, H. Grönbeck, A. Lloyd Spetz, M. Eriksson, and M. Skoglundh, *J. Phys. Chem. B* **109**, 9581 (2005).
- ³⁰C. H. Bartholomew, P. K. Agrawal, and J. R. Katzer, *Adv. Catal.* **31**, 135 (1982).
- ³¹T. E. Fischer and S. R. Kelemen, *J. Catal.* **53**, 24 (1978).
- ³²N. Barbooth and M. Salame, *J. Catal.* **104**, 240 (1987).
- ³³J. A. Rodriguez and J. Hrbek, *Acc. Chem. Res.* **32**, 719 (1999).
- ³⁴A. K. Neyestanaki, F. Klingstedt, T. Salmi, and D. Y. Murzin, *Fuel* **83**, 395 (2004).
- ³⁵S. Dhar, S. R. Wang, and J. R. Williams, *MRS Bull.* **30**, 288 (2005).
- ³⁶R. N. Ghosh and R. Loloee (unpublished).
- ³⁷H. P. Bonzel and R. Ku, *J. Chem. Phys.* **58**, 4617 (1973).
- ³⁸W. Heegemann, K. H. Meister, E. Bechtold, and K. Hayek, *Surf. Sci.* **49**, 161 (1975).
- ³⁹D. E. Kuhl and R. G. Tobin, *Rev. Sci. Instrum.* **66**, 3016 (1995).
- ⁴⁰R. L. Summers, NASA Technical Note No. TND-5285 (1969) (unpublished).
- ⁴¹Y. Berthier, M. Perdereau, and J. Oudar, *Surf. Sci.* **36**, 225 (1973).
- ⁴²R. J. Koestner, M. Salmeron, E. B. Kollin, and J. L. Gland, *Surf. Sci.* **172**, 668 (1986).
- ⁴³H. P. Bonzel and R. Ku, *J. Chem. Phys.* **59**, 1641 (1973).
- ⁴⁴V. D. Thomas, J. W. Schwank, and J. L. Gland, *Surf. Sci.* **501**, 214 (2002).
- ⁴⁵The molecular weight of H₂S (34 amu) coincides with that of the oxygen isotope ¹⁶O¹⁸O, which is present in the oxygen gas at a level of about 0.4%. When the oxygen partial pressure was high enough for the isotope signal to be significant, it was measured before the H₂S exposure and subtracted from the mass 34 signal to determine the actual H₂S level.
- ⁴⁶U. Köhler, M. Alavi, and H.-W. Wassmuth, *Surf. Sci.* **136**, 243 (1984).
- ⁴⁷S. Astegger and E. Bechtold, *Surf. Sci.* **122**, 491 (1982).
- ⁴⁸A. Michaelides and P. Hu, *J. Chem. Phys.* **115**, 8570 (2001).
- ⁴⁹A. Güttler, D. Kolovos-Vellianitis, T. Zecho, and J. Küppers, *Surf. Sci.* **516**, 219 (2002).
- ⁵⁰N. S. Nasri, J. M. Jones, V. A. Dupont, and A. Williams, *Energy Fuels* **12**, 1130 (1998).
- ⁵¹U. Köhler and H.-W. Wassmuth, *Surf. Sci.* **117**, 668 (1982).
- ⁵²H. Hopster, H. Ibach, and G. Comsa, *J. Catal.* **46**, 37 (1977).
- ⁵³A. Winkler, X. Guo, H. R. Siddiqui, P. L. Hagans, and J. T. Yates, Jr., *Surf. Sci.* **201**, 419 (1988).
- ⁵⁴A. Rar and T. Matsushima, *Surf. Sci.* **318**, 89 (1994).
- ⁵⁵H. Wang, R. G. Tobin, D. K. Lambert, C. L. DiMaggio, and G. B. Fisher, *Surf. Sci.* **372**, 267 (1997).